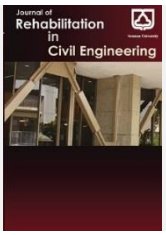

Journal of Rehabilitation in Civil Engineering

Journal homepage: https://civiljournal.semnan.ac.ir/

Flexural Behavior of UHPC Beams Reinforced with Macro-Steel Fibers and Different Ratios of Steel and GFRP Bars

Yousof Abbasi Parvin [1]; Taleb Moradi Shaghaghi [1]; Masoud Pourbaba [2,*]; Seyed Saeed Mirrezaei [1]; Yousef Zandi [1]

1. Department of Civil Engineering, Tabriz Branch, Islamic Azad University, Tabriz, Iran
2 Department of Civil Engineering, Maragheh Branch, Islamic Azad University, Maragheh, Iran

* Corresponding author: Ph.D., E-mail: *pourbaba@iau-maragheh.ac.ir*

ARTICLE INFO

Article history:
Received: 11 August 2022
Revised: 01 January 2023
Accepted: 05 July 2023

Keywords:
Flexural and shear behavior;
GFRP;
Steel fiber;
UHPFRC.

ABSTRACT

The flexural and shear behavior of ultra-high-performance fiber-reinforced concrete (UHPFRC) reinforced with different ratios of glass-fiber-reinforced polymer (GFRP) and conventional steel rebars is experimentally studied in this paper. For this purpose, three beams with dimensions of 250×300×1650 mm were reinforced with GFRP rebars in three different ratios (0.64%, 1.05%, and 1.45%) and hooked-end (H) steel fibers by 2% volumetric ratio. Similar procedure was carried for beams reinforced with conventional rebars. Additionally, Nonlinear regression analyses were also carried out to simulate the flexural load-deflection behavior of the beams. Results showed that the role of hooked-end fibers in compensating for the brittle nature of GFRP rebars was insignificant. Besides, increase of the longitudinal reinforcement ratio changed the failure mode from flexural to shear failure in specimens with GFRP rebars. Finally, nonlinear regression models were proposed that successfully capture the load-deflection behavior of the test specimens with coefficient of correlation (R^2) very close to unity.

E-ISSN: 2345-4423

How to cite this article:
Abbasi Parvin, Y., Moradi Shaghaghi, T., Pourbaba, M., Mirrezaei, S. S., & Zandi, Y. (2024). Flexural Behavior of UHPC Beams Reinforced with Macro-Steel Fibers and Different Ratios of Steel and GFRP Bars. Journal of Rehabilitation in Civil Engineering, 12(2), 41-57. https://doi.org/10.22075/jrce.2023.28070.1695

1. Introduction

Since concrete introduction in 1800s, it has become the most common construction material which has gone through dramatic changes both in its chemical composition and fabrication methods to meet the requirements of field applications throughout the world. However, despite its ubiquitous use, concrete suffers from a notable disadvantage, that being its brittleness and weak performance in tension [1]. To remedy this disadvantage, and to account for the ever-growing need for efficient and resilient structures, a new class of cementitious materials known as ultra-high-performance concrete (UHPC) has been developed in recent years. UHPC has superior performance compared to its conventional strength counterpart. Hence, applications of UHPC are multifaceted and it is used in high performance composite structures, very slender structures, and in new important structures and infrastructures.

To resolve the issue of brittleness in UHPC, steel, synthetic, mineral and natural fibers were incorporated into UHPC [2]. Among the so-called fibers, steel fibers, owing to their excellent tensile strength and stiffness have shown to be a promising supplementary material to concrete which greatly enhance its performance in tension. In this regard, as mentioned above, because of promising specification of ultra-high performance fiber-reinforced concrete (UHPFRC), research has been carried out to characterize its behavior under different loading scenarios and ambient conditions such as effect of age and curing regimes [3,4], tension, shear and flexural performance [5-10], pullout response [11-16], fracture parameters [7].

In concrete structures, steel rebars are generally used to overcome the brittleness and low tensile strength of concrete. However, for many reinforced concrete structures exposed to aggressive environments, chloride causes corrosion of steel rebars. Therefore, in order to overcome the corrosion problem in reinforced concrete, the development of new materials has accelerated in recent years. One of these materials is fiber reinforced polymer (FRP) rebars. Some other advantages of FRP rebars such as, high tensile strength, light weight, high fatigue resistance, electrical insulation, non-magnetic, creep deformation, have caused some structural designers and researchers to use of them as a suitable substitute for steel rebars in various concrete structures in recent years [8]. However, in spite of the advantages of FRP rebars compared to the reinforcement of convention steel rebars, due to the various differences in mechanical and physical properties between the two materials (tensile strength, modulus of elasticity, continuity between concrete and rebars, etc.), replacement of them with steel rebars required laboratory research and observing the behavior of FRP rebars in combination with concrete. Yoo et al. (2016) studied the flexural behavior of UHPFRC beams with GFRP bars and the combined reinforcement of GFRP and steel rebars. The result of tests showed that partial replacement of GFRP bars with steel rebars causes post cracking stiffness improvement but lower deformability [9]. Ahangarnazad et al. (2020) studied both numerically and experimentally the bond behavior between steel and GFRP bars, and UHPC showed that the steel rebars have higher bond strength compared with GFRP bars in UHPC [10]. De Sá et al. (2020) investigated the flexural behavior of concrete specimens reinforced with macro polypropylene (PP) fibers and GFRP bars; the results were compared with their plain concrete counterpart. Results showed that the performance of the PP fibers in increasing the ductility of the beams were the most favorable with increases up to 162% [11]. Dev et al. (2020) studied the shear behavior of thirteen RC specimens which served as structural bridge elements with

GFRP rebars subject to shear or a combination of shear and bending loading [12]. Patil et al. (2020) tested fourteen GFRP reinforced concrete beams with the inclusion of polyolefin (PO) and hybrid fibers under flexural loading [13].

Liu et al. (2022) investigated the flexural behavior of reinforced concrete beams with FRP and conventional steel rebars. The results indicated that concrete beams with BFRP and steel bars resulted to large deflections and crack widths during the loading process [14]. El-Sayed and Algash (2022) studied the flexural behavior of the UHPC beams reinforced with glass fiber reinforced polymer (GFRP) bars was studied. Their results showed that using GFRP bars resulted to ultimate load carrying capacity. GFRP beams also, showed a smaller deflection increase at the same ultimate load. The beams reinforced with GFRP bars had a higher crack width compared with control [15]. Betschoga et al (2021) studied the shear behavior of concrete beams with different boundary and loading conditions. They investigated various parameters such as simply supported and cantilever beams using some difference loading conditions such as concentrated and uniformly distributed loads. They concluded that there are notable differences with regard to the location of the critical shear crack and the shear resistance in the specimens which they have tested [16].

In line with the need for resilient and light structures, glass fiber-reinforced polymers have become the focus of attention during recent years with favorable characteristics such as low weight when compared to conventional rebars and good resistance to corrosion. Even so, glass-GFRPs do not show a ductile behavior before failure therefore investigation of GFRPs bars behavior in combination of concrete is necessary. It should be noted that in most of the former studies, the behavior of FRP-RC beams with strength in the range of 20-80 MPa has been studied. On the other hand, due to the introduction and development of UHPFRC concretes as the strongest concretes in the world today with compressive strength above 130 MPa, there is still no more research on the behavior of FRP-UHPFRC beams to evaluate their performance under different conditions.

Table 1. Mix proportions.

Mix	Proportion of materials per $\boldsymbol{kg/m^3}$							
	Portland Cement	Silica Fume	Sand	Gravel	Quartz Powder	W/C	Superplasticizer	Steel Fiber
UHPFRC	722	228	992	---	206	0.24	60	151

Table 2. Properties of hooked-end steel fibers.

$\boldsymbol{d_f}$ (mm)	$\boldsymbol{L_f}$ (mm)	$(\boldsymbol{L_f/d_f})$	Density (g/$\boldsymbol{cm^3}$)	$\boldsymbol{f_t}$(MPa)	$\boldsymbol{E_f}$(GPa)
0.8	30	37.5	7.5	1900	200

d_f = Diameter, L_f = Length, f_t = Tensile strength and E_f = Elastic modulus

With this in mind, this research investigates the possible feasibility of improving the brittle nature of GFRP rebars by adding hooked-end steel fibers to UHPC concrete mixes and also draws comparisons with specimens reinforced with conventional steel rebars.

2. Experimental program

2.1. Materials

The mix for UHPFRC consisted of Type II Portland Cement, silica fume with a maximum dimension of 229 μm, polycarboxylate-based

ether (e.g., AURAMIX) as superplasticizer, fine sand sifted through No. 16 sieve (less than 1.1 mm), quartz powder and hooked-end steel fibers with a length of 30 mm, diameter of 0.8 mm and tensile strength of 1900 MPa [17]. Table 1 and 2 shows UHPFRC mix proportions and specifications of hooked-end fibers.

2.2. Compression tests

A series of compression tests were tested on 100×100 mm cube. The average compressive strength of UHPFRC specimens was 130 MPa.

2.3. Modulus of elasticity tests

Modulus of elasticity tests were carried out according to ASTM C469/C469M-14 [18], on cylindrical specimens with dimensions of 150×300 mm and calculations were performed based on the results obtained for the average of three specimens as follows:

$$E_c = \frac{0.4f_c' - f_{c1}}{\varepsilon_2 - 0.00005} \quad (1)$$

Where, E_c is the modulus of elasticity of the concrete; f_c' and f_{c1} are the compressive stress corresponding to strain ε_2 and an axial strain of 0.00005 respectively. Three LVDTs were used to monitor and record the axial strains over the height of the cylinder as shown in Fig. 1.

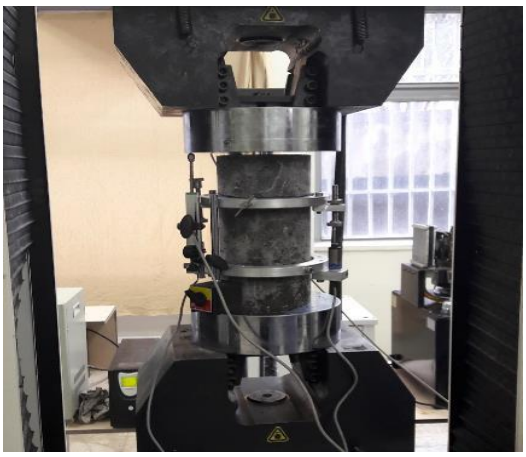

Fig. 1. Modulus of elasticity experiment.

Some methods have been presented for predicting the Modulus of elasticity reinforced. Some of these equations are given in Table 3.

Fig. 2. Curing of specimens.

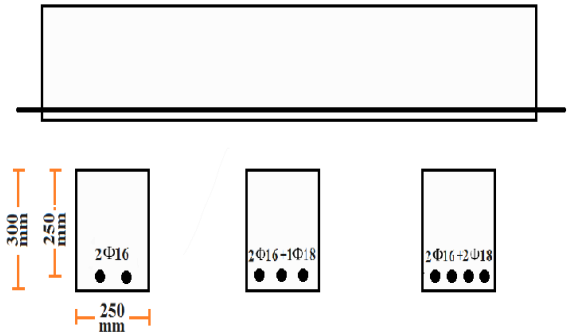

Fig. 3. Detailing of reinforcements.

2.4. Flexural tests

In this study, Indirect/flexure tests were done considering ASTM C1609/C1609M [19]. For this purpose six UHPFRC beam specimens with of the 250×300×1650 mm dimensions fabricated. Fig. 4 and 5 show the curing and details of specimens are shown in respectively.

Tests were performed at a rate of 0.5 mm/min in a displacement control manner, with LVDTs recording mid-span displacements. Three beams reinforced with GFRP rebars in three different ratios (0.64%, 1.05%, and 1.45%) and hooked-end (H) steel fibers by 2% volumetric ratio were cast. A similar procedure was carried out for their counterpart with conventional steel rebars. Specifications of rebars and their layout are given in Tables 4 and 5 and Fig. 4 shows test setup of specimens.

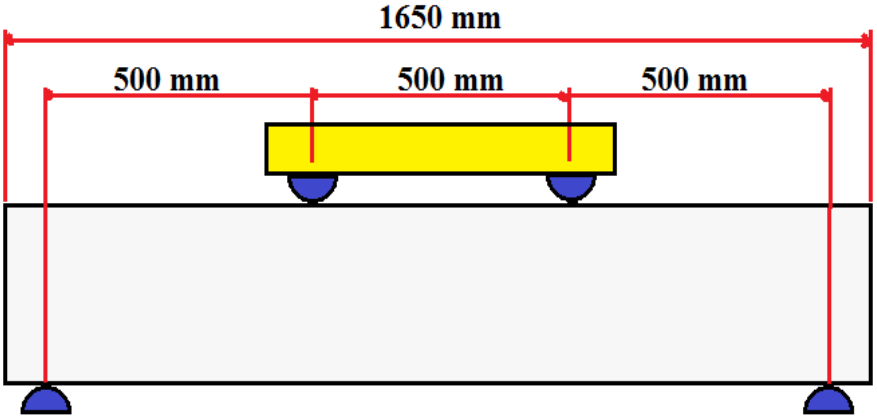

Fig. 4. Dimensions and test setup of specimens.

Table 3. Available equations in the literature for the modulus of elasticity of UHPFRC.

Researcher(s)	Equations (unit: GPa)	Note	Ref
Kollmorgen (2004)	$E_c = 11800(f_c')^{\frac{1}{3.14}}$	$34 \leq f_c' \leq 207$ MPa	[20]
KCI (2007)	$E_c = 8500\sqrt[3]{f_c' + 8}$	---	[21]
Graybeal (2007)	$E_c = 3840\sqrt{f_c'}$	$126 \leq f_c' \leq 193\ MPa$	[22]
Graybeal & Stone (2012)	$E_c = 4069\sqrt{f_c'}$	$97 \leq f_c' \leq 179\ MPa$	[23]
Lee et al. (2015)	$E_c = (-367V_f \frac{l_f}{d_f} + 5520){f_c'}^{0.41}$	---	[24]
Alsalman et al. (2017)	$E_c = 8010(f_c')^{0.36}$	$31 \leq f_c' \leq 235\ MPa$	[25]
Haber et al. (2018)	$E_c = 3755\sqrt{f_c'}$	$64.8 \leq f_c' \leq 153\ MPa$	[26]
Suksawang et al. (2018)	$E_c = 4700\lambda\sqrt{f_c'}$	$\lambda = (1 + 0.7^{V_f})/2$	[27]
Current study	---	$f_c' = 130\ MPa, E_c = 42.91\ GPa$	

Table 4. Properties of steel and GFRP rebars.

Reinforcement	E (GPa)	f_y (MPa)	f_u(MPa)
Steel	200	400	600
GFRP	60	N.A	1000

E = Modulus of elasticity of reinforcement;

f_y = Specified yield strength of reinforcement;

f_u= Ultimate tensile strength of reinforcement

Table 5. Details of specimens.

ID	Type	f_c'(MPa)	Type of rebar	No. of rebars	ρ(%)
UH-F-0.64	UHPFRC	130	GFRP	2φ16	0.64
UH-F-1.05	UHPFRC	130	GFRP	2φ16+1φ18	1.05
UH-F-1.45	UHPFRC	130	GFRP	2φ16+2φ18	1.45
UH-S-0.64	UHPFRC	130	Steel	2φ16	0.64
UH-S-1.05	UHPFRC	130	Steel	2φ16+1φ18	1.05
UH-S-1.45	UHPFRC	130	Steel	2φ16+2φ18	1.45

3. Results

3.1. Modulus of elasticity

Fig. 5 shows the average stress-strain curve of cylindrical specimens. Comparison of the obtained average value of 42.91 GPa with the values predicted from available equations, Table 6, shows that these equations mainly estimate the modulus of elasticity reasonably with a 10% margin of error except for the equation proposed by Kollmorgen (2004) which significantly overestimates modulus of elasticity (30%) [20]; the equation proposed by Haber et al. (2018) gives the best estimation [26]. Other comparisons are given in Table 6.

3.2. Flexural results

Figs. 6(a)-6(c) show crack patterns of specimens with GFRP rebars under four-point bending tests, highlighting the importance of fibers in preventing full separation of the two sections.

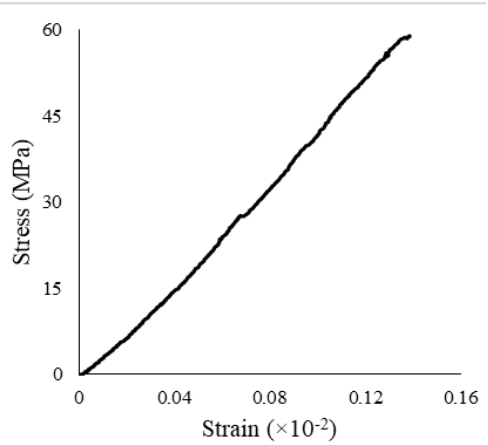

Fig. 5. Stress-strain curve to determine modulus of elasticity.

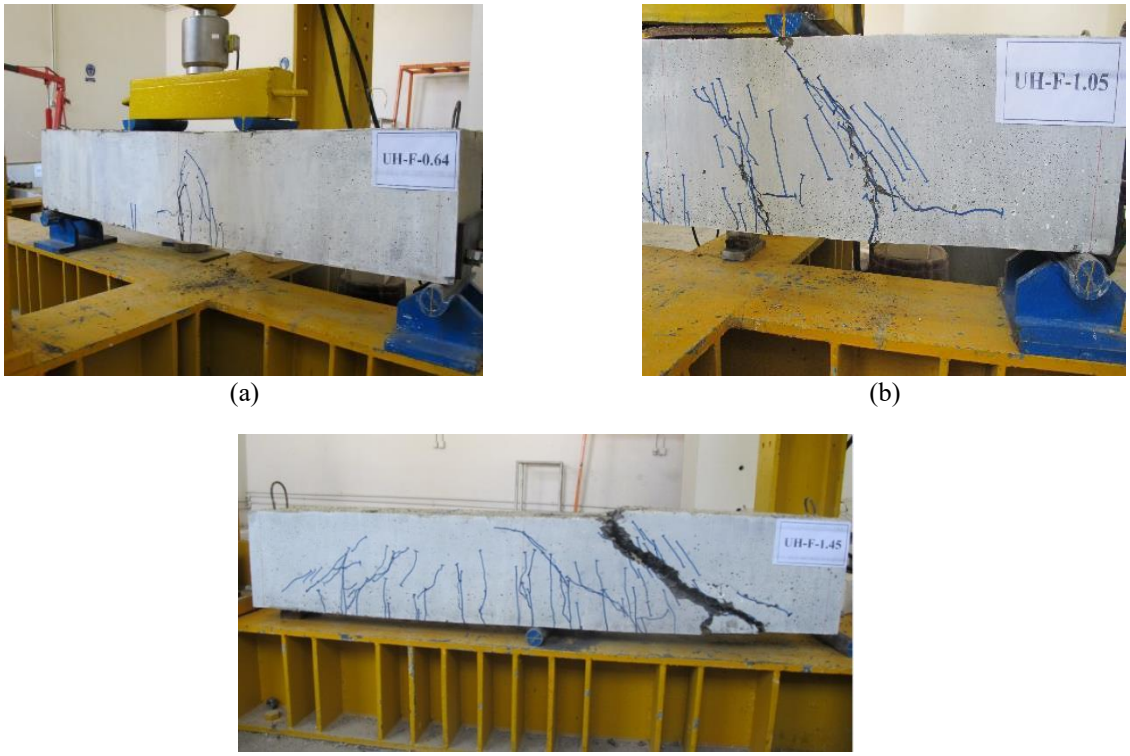

(a) (b)

(c)

Fig. 6. Crack pattern of specimens with GFRP rebars (a) UH-F-0.64, (b) UH-F-1.05, (c) UH-F-1.45.

Four-point bending tests are generally preferred as they provide a sizeable region with a uniformly distributed maximum bending moment, hence avoiding problems such as stress concentration in crack patterns. This in part explains why critical cracks in Figs. 6(a)-6(c) are not exactly at the mid-section of the beam. Moreover, despite their similar sizes, peak loads in four-point bending tests are 50% higher than those in three-point bending tests so as to develop comparable moments.

Comparison of Figs. 6(a)-6(c) show that with the increase in longitudinal reinforcement ratio, crack pattern shifts from flexural behavior towards shear behavior which is clearly visible in Fig. 6(c). Increasing the reinforcement ratio from 0.64% to 1.05% and from 1.05% to 1.45% led to an increase of 9% and 15% in load-bearing capacity of the beams. This increase was much more significant for their conventional steel rebars with increases being 44% and 30%.

It is also noteworthy that for a given longitudinal reinforcement ratio peak load values for specimens with GFRP rebars are notably higher than their conventional steel rebar counterparts especially at low reinforcement ratios (64%) compared to two medium reinforcement ratios (25% and 11%, respectively for 1.05% and 1.45% reinforcement ratios). On the other hand, however, hooked-end steel fibers had only limited crack widening and have not contributed to ductility of specimens and the brittle nature of GFRP rebars dictates the failure mode.

Similarly, Figs. 7(a)-7(c) for specimens with conventional steel rebars, do not show a particular failure trend and generalization cannot be made with regard to the failure mode of the specimen being dependent on reinforcement ratio of conventional steel rebars. However, in contrary to specimen with GFRP rebars, a ductile pattern was observed for these specimens. Figs, 8(a) and 8(b) support the observations in Figs. 6 and 7.

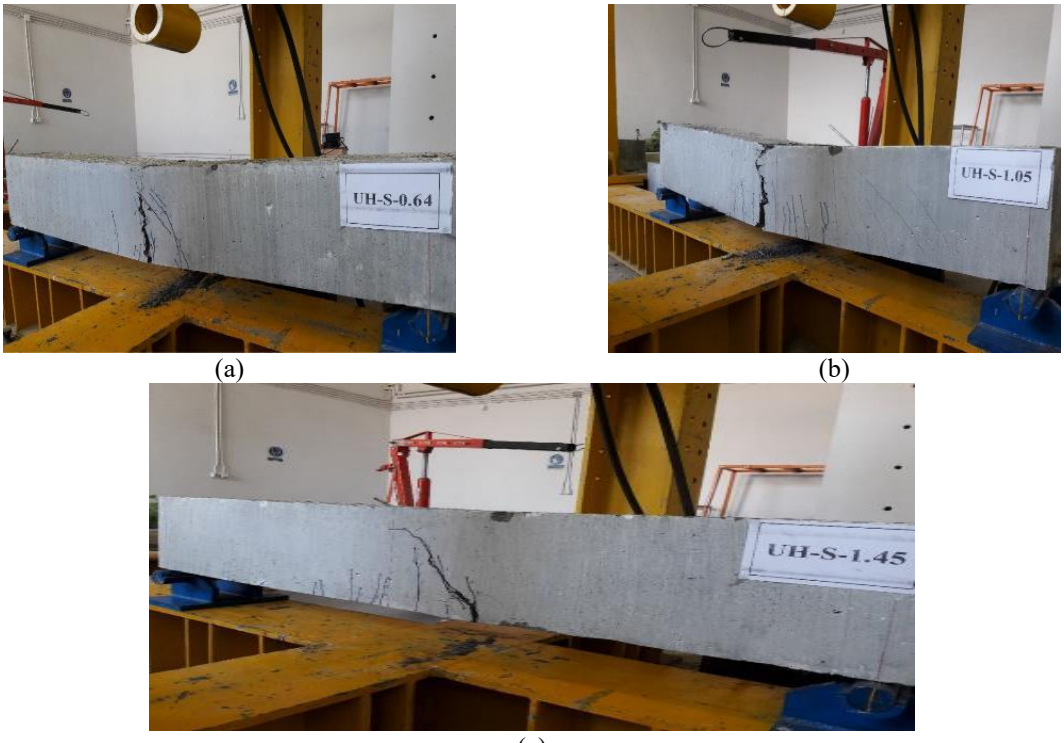

(a) (b)

(c)

Fig. 7. Crack pattern of specimens with conventional steel rebars (a) UH-S-0.64, (b) UH-S-1.05, (c) UH-S-1.45.

Table 6. Ratio of experimental modulus of elasticity to calculated from equations.

$E_{c-test}(GPa)$	E_{c-test}/E_{c-calc}							
	Kollmorgen (2004) [20]	KCI (2007) [21]	Graybeal (2007) [22]	Graybeal & Stone (2012) [23]	Lee et al. (2015) [39]	Alsalman et al. (2017) [25]	Haber et al. (2018) [26]	Suksawang et al. (2018) [42]
42.91	1.30	1.02	1.02	1.08	0.90	1.08	1.00	0.93

What's more, compared to peak load values, peak load deflections were more sensitive to variations in longitudinal reinforcement ratio (see Fig. 9), i.e., peak load deflections saw a 4% and 24% increase for specimens with GFRP rebars and 25% and 32% for specimens with conventional steel rebar.

3.3. Fracture energy

Fig. 10 and 11 shows that with the increase in reinforcement ratio, regardless of its type, fracture energy increases. Nonetheless, this increase is more pronounced in specimens with conventional steel rebars as they show a ductile plastic pattern after the yield stress is reached, while on the other hand specimen with GFRP rebars are characterized by a brittle failure after the peak load is reached. Moreover, it can be seen that a linear trend exists between the fracture energy of the specimens in different mid-span deflection values (Fig. 12) and as expected based on Figs. 8(a) and 8(b), the sensitivity of this parameter is higher for specimens with conventional steel rebars when compared to their GFRP counterparts.

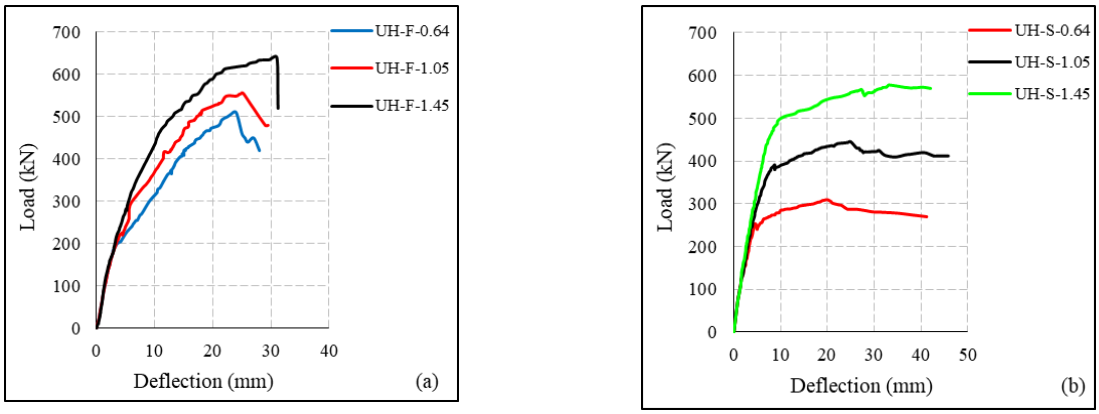

Fig. 8. Load-deflection curves (a) specimens with GFRP rebars (b) specimens with conventional steel rebars.

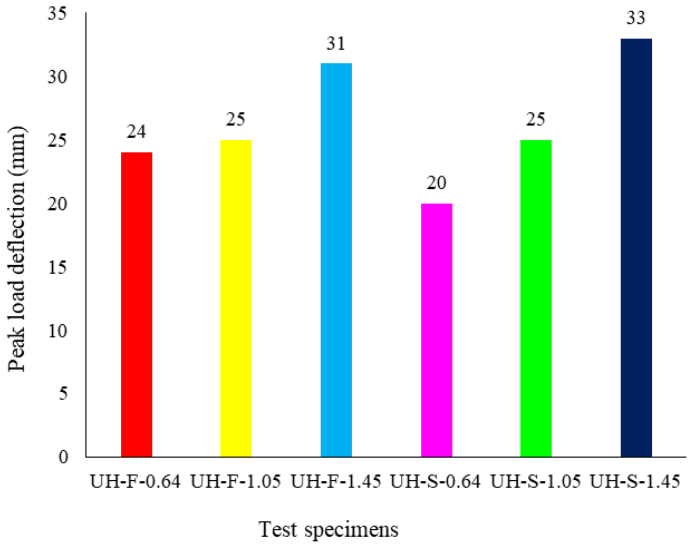

Fig. 9. Comparison of deflections corresponding to the peak load.

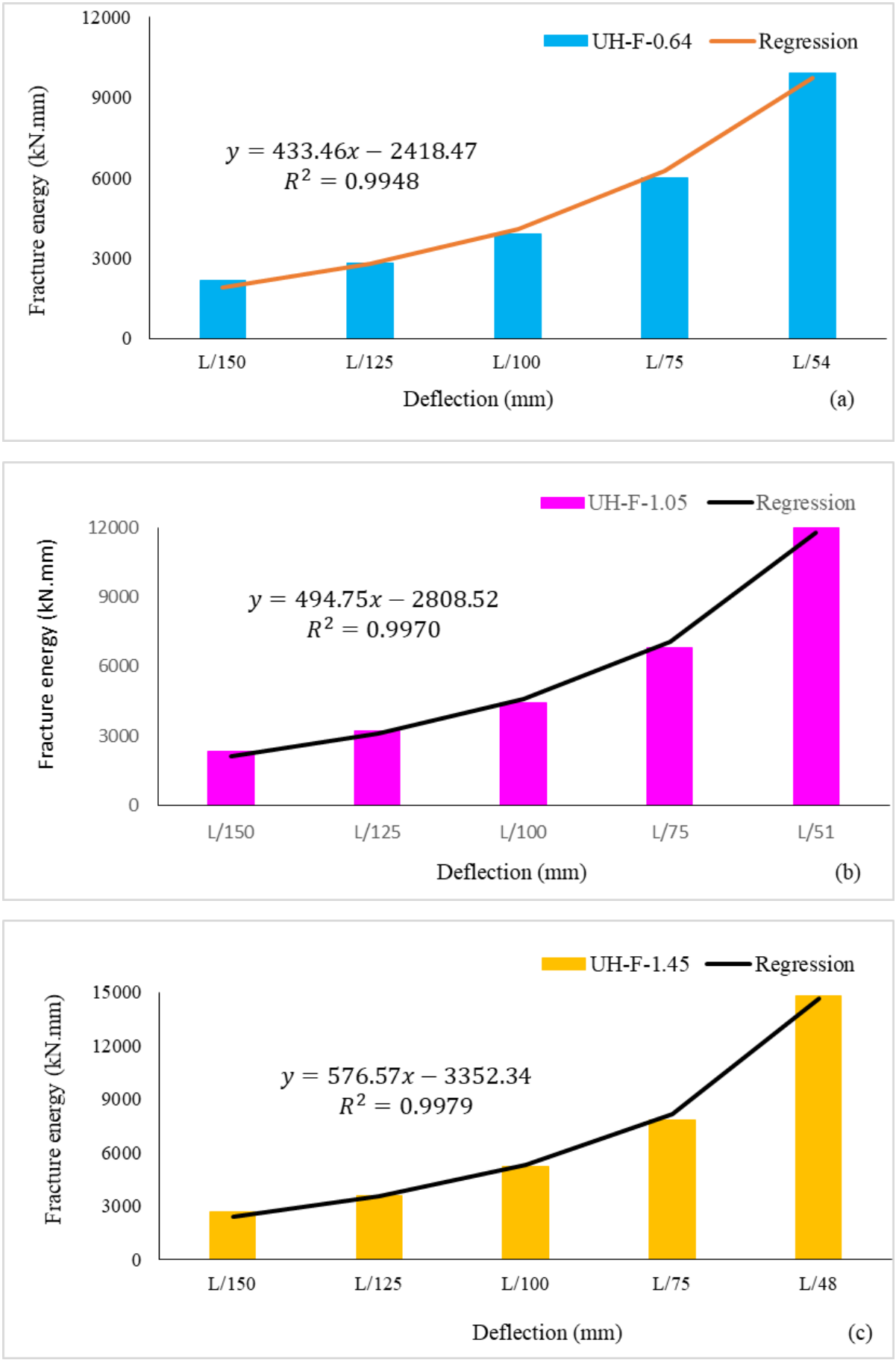

Fig. 10. Fracture energy of specimens (a) UH-F-0.64, (b) UH-F-1.05, (c) UH-F-1.64.

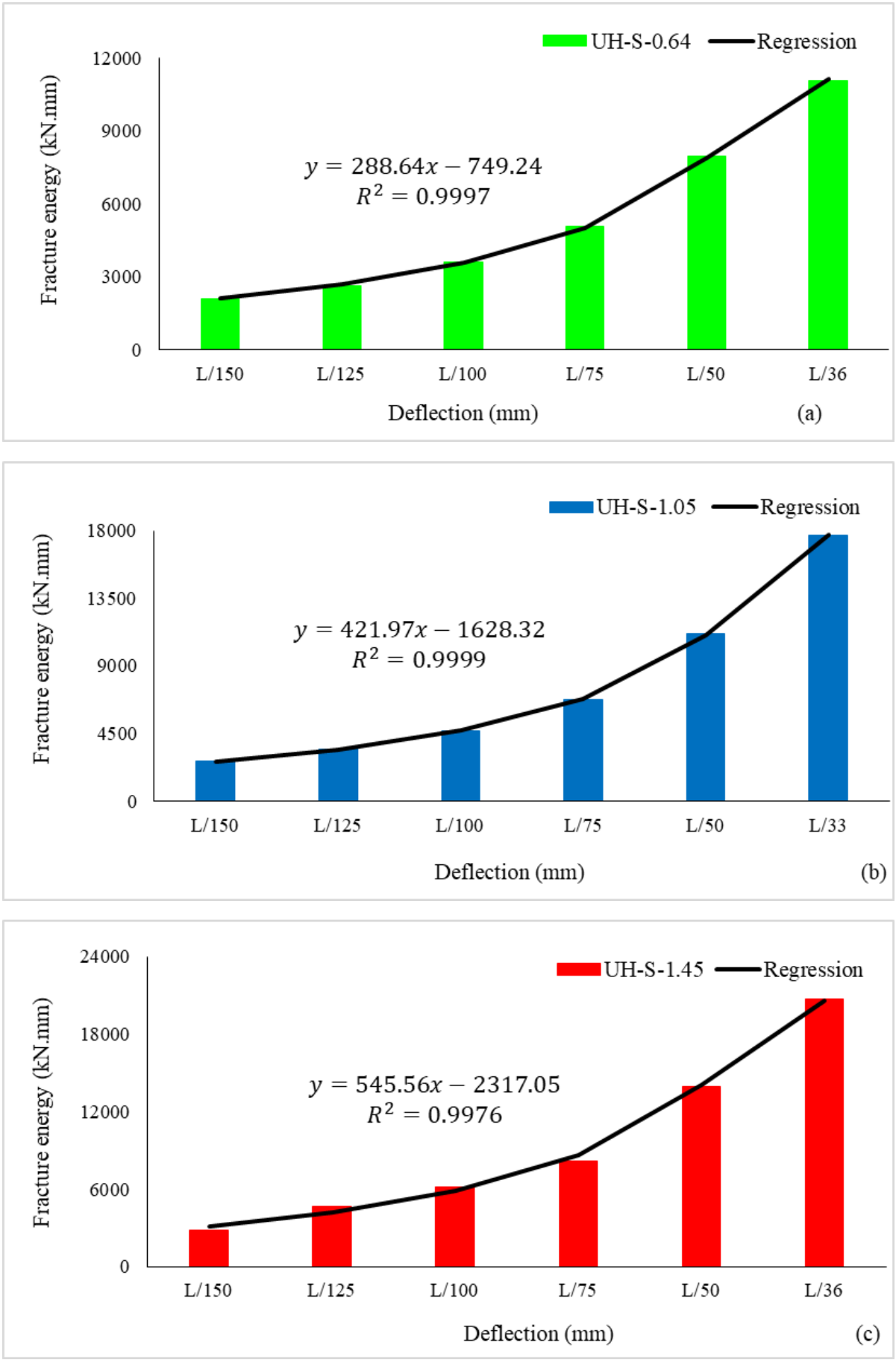

Fig. 11. Fracture energy of specimens (a) UH-S-0.64, (b) UH-S-1.05, (c) UH-S-1.

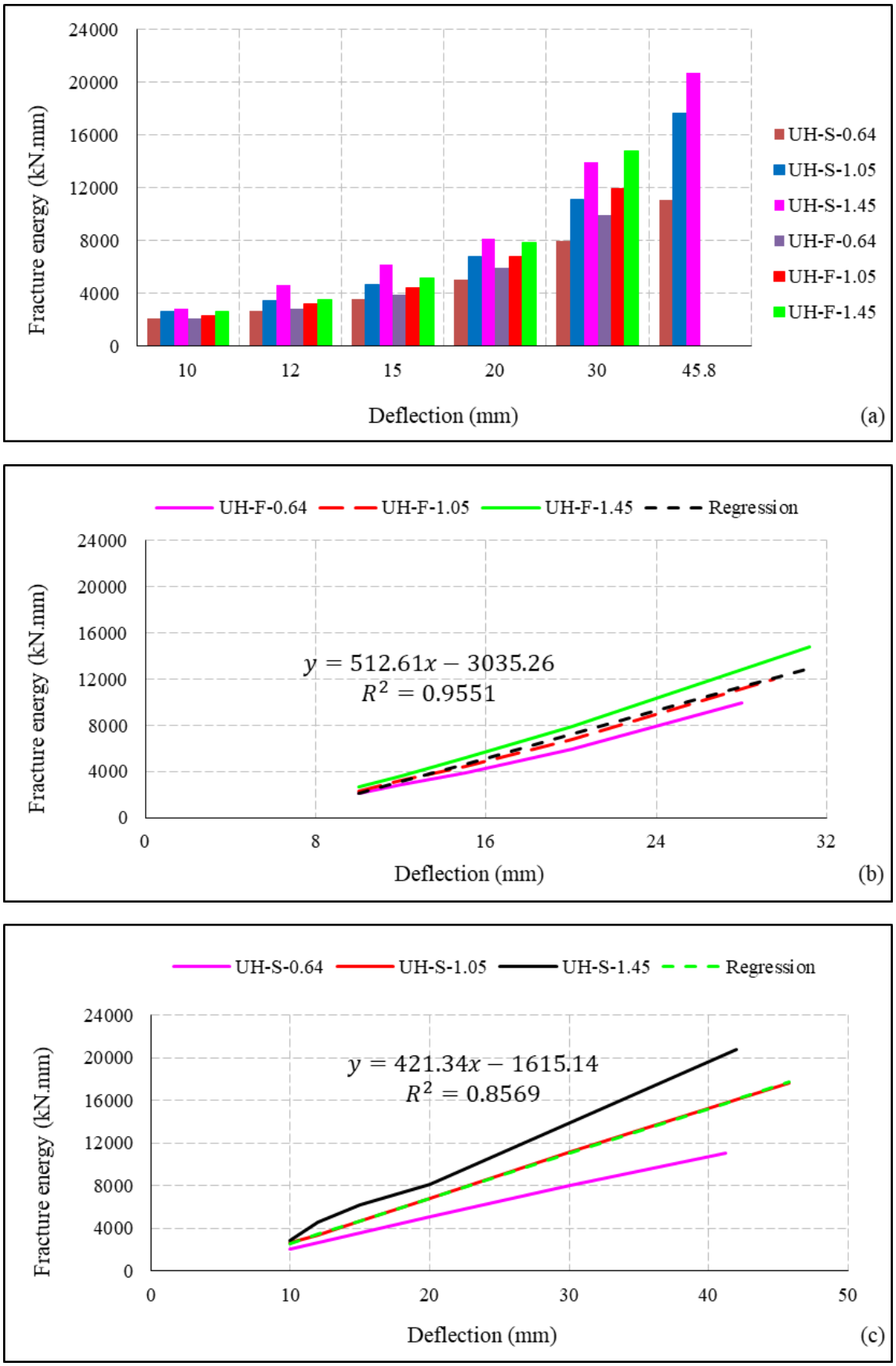

Fig. 12. Fracture energy of specimens at various mid-span deflection values (a) all the specimens (b) regression model for specimens with GFRP rebars (c) regression model for specimens with conventional steel rebars.

This can be justified by the very fact that a large proportion of the energy is absorbed in the post-yield region of the curves which is significant in conventional steel rebars and the share of the linear region is insignificant. Furthermore, validation of this issue can be implied from the value of the coefficient of correlation and the residual value for fracture energy according to Fig. 13 (i.e., variation of residuals is more pronounced in specimens with conventional steel rebars).

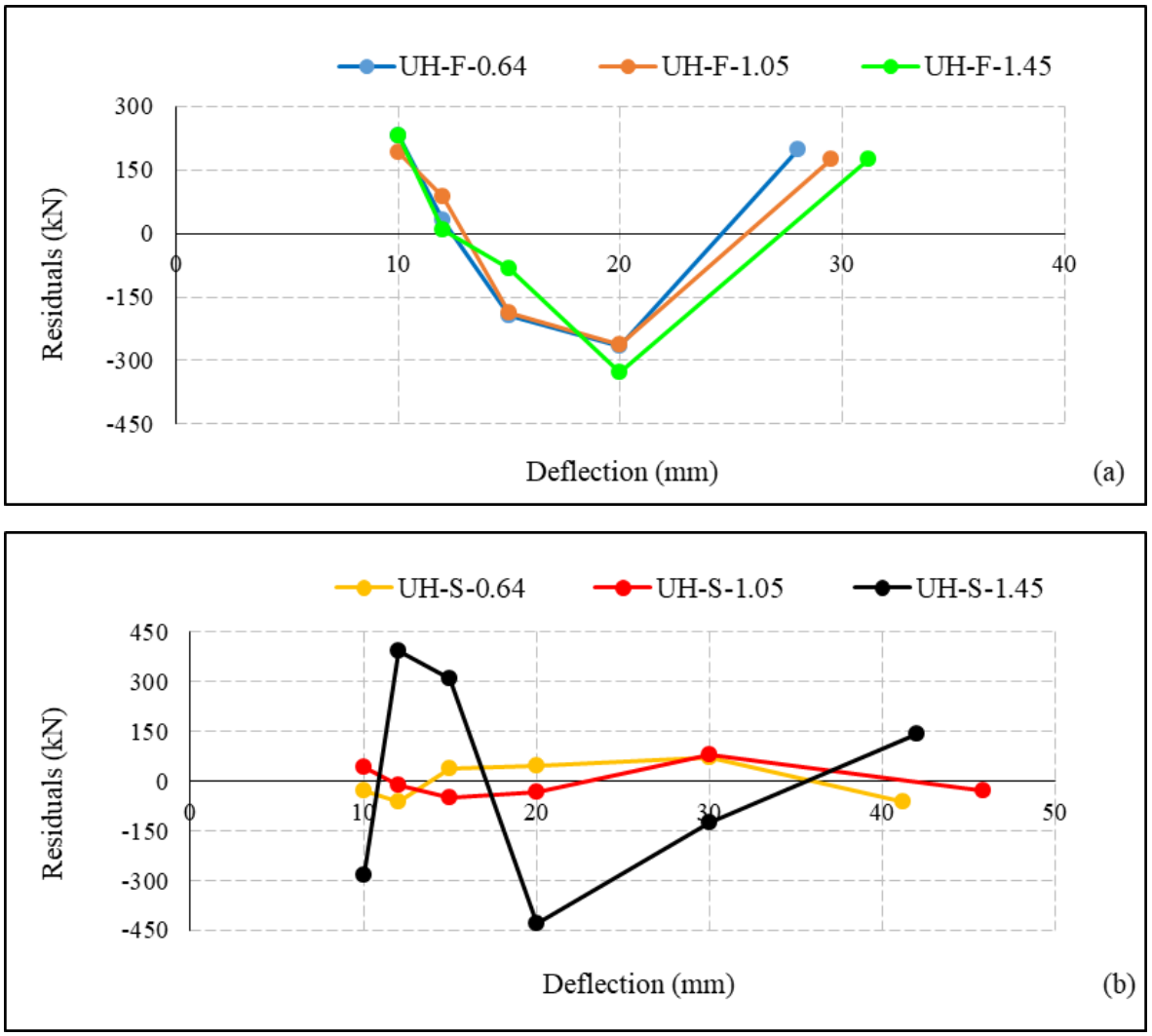

Fig. 13. Residuals for the predicted and estimated values in regression analyses for fracture energy (a) specimens with GFRP rebars (b) specimens with conventional steel rebar.

3.4. Nonlinear regression analyses

Based on the obtained load-displacement curves for prismatic beam specimens, a model is suggested to estimate the experimental load-deflection curves as follows:

$$y = \frac{a+bx}{1+cx+dx^2} \quad (2)$$

Where, x is the ratio of the given deflection to the deflection corresponding to the peak load and y is the ratio of the given load to the peak load. a, b, c and d are the fitting parameters obtained from nonlinear regression analyses, the values of which for test specimens are given in Table 7.

Similarly, corresponding fitting curves are also presented in Figs. 14. It can be seen that experimental and statistical-based curves correlate very well with one another with coefficient of determination values over 0.95.

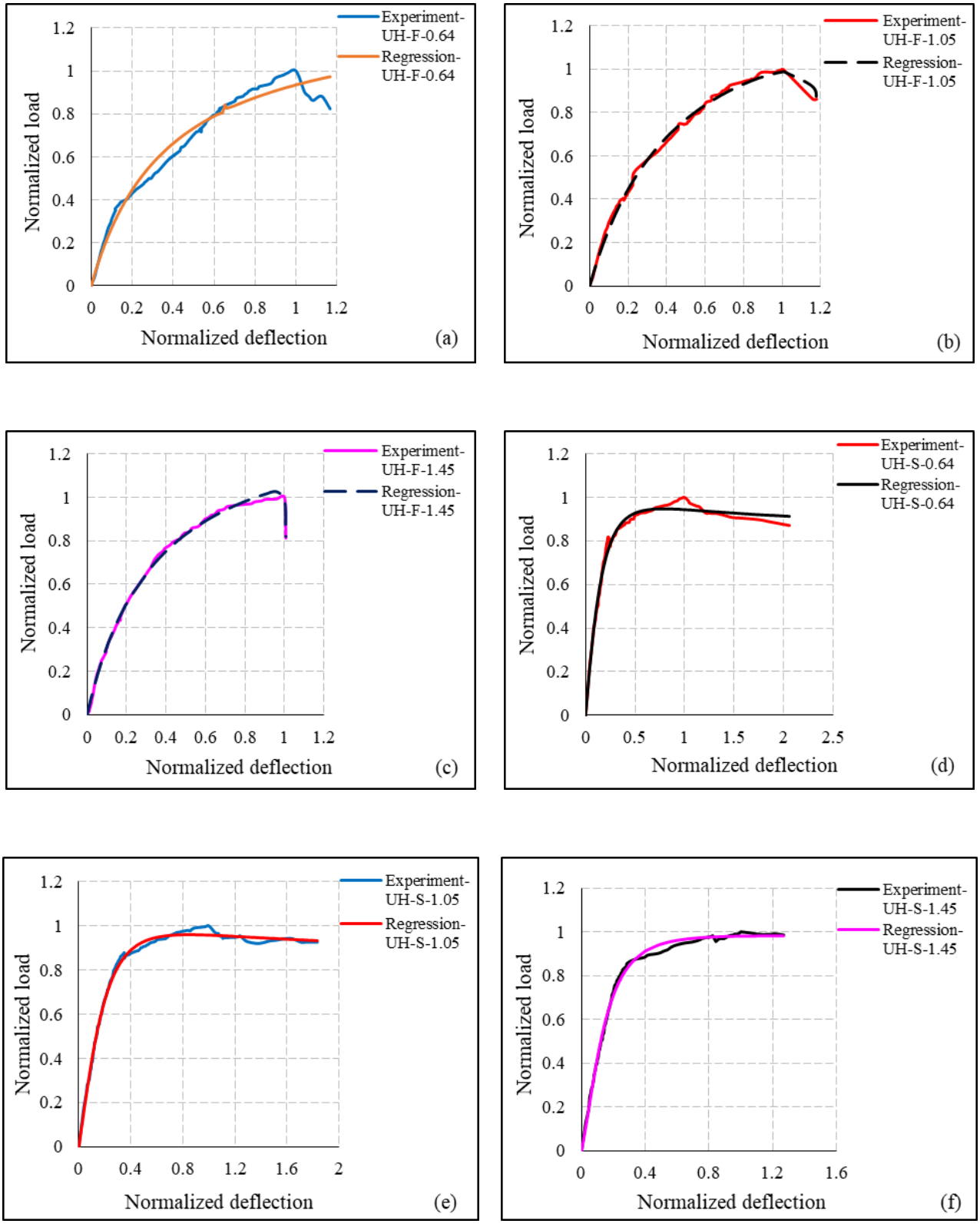

Fig. 14. Nonlinear regression analyses (a) UH-F-0.64, (b) UH-F-1.05, (c) UH-F-1.64, (d) UH-S-0.64, (e) UH-S-1.05, (f) UH-S-1.6.

Further criteria regarding the goodness of fit can be evaluated using the two well-known criteria, namely standard deviation (STEDV, equation (3)) and root mean square error (RMSE, equation (4)). The former criteria serve as how the data have scattered around the mean value while the latter quantifies the scatter of the scatter of the predicted data relative to the experimental values. According to Table 7, values for STDEV for the experimental values and regression analyses are very close to one another (margin of error less than 2%). Similar trend is observed for the RMSE values for which proximity to zero denotes better results. As evident from Table 7, these values are very close to zero and therefore the statistical nonlinear regression analyses are validated based on three criteria.

$$STDEV = \sqrt{\frac{\sum_{i=1}^{n}(x_i-\bar{x})^2}{n-1}} \quad (3)$$

$$RMSE = \sqrt{\frac{\sum_{i=1}^{n}(x_i-\hat{x}_i)^2}{n}} \quad (4)$$

Where, x_i are the observations, $\bar{x}$ mean of the observations, $\hat{x}_i$ predicted values based on regression analyses, and n the number of observations available for analysis.

Table 7. Fitting parameters for load-deflection curves.

Sample ID	a	b	c	d	R^2	STDEV (Experiment)	STDEV (Regression)	RMSE
UH-F-0.64	3.4224	-5.2624	1.1243	-4.0923	0.9841	0.2918	0.2936	0.0367
UH-F-1.05	3.1809	-2.6302	1.2992	-1.7413	0.9965	0.2986	0.3019	0.0175
UH-F-1.45	4.0134	-3.9806	1.8391	-2.8059	0.9983	0.3221	0.3186	0.0130
UH-S-0.64	5.4683	12.9006	3.2327	15.2332	0.9886	0.2274	0.2256	0.0241
UH-S-1.05	4.0472	11.2726	1.8526	13.1348	0.9958	0.2496	0.2492	0.0161
UH-S-1.45	3.6368	26.3920	2.0400	27.5903	0.9975	0.2876	0.2881	0.0141

4. Conclusions

This research presents and experimental study on six UHPC beams reinforced with different ratios of GFRP and conventional steel rebars as well as hooked-end steel fibers by 2% volumetric ratio. Compression and flexural tests were carried out on the specimens and results were discussed in previous sections. The salient point of the study can be summarized as follows:

For the specimens tested in the current study, equations available in the literature provided a reasonably favorable estimation of the modulus of elasticity with a margin of error less than 10% except for the equation proposed by Kollmorgen (2004) which overestimate modulus of elasticity by 30% [20].

Despite the inclusion of the hooked-end steel fibers, their role in remedying the brittle nature of GFRP specimens was insignificant.

Reinforcement ratio highly affected the results (especially for specimens with conventional steel rebars) with the load capacity increasing with the increase in the ratio. This increase was more notable for specimens with

conventional steel rebars, i.e., 44% and 30% increase for specimens UH-S-1.05 and UH-S-1.45 compared to specimen UH-S-0.64. For specimens reinforced with GFRP rebars, similar values were 9% and 15% for low reinforcement ratios, flexural behavior governed the behavior and this pattern shifted towards shear failure with the increase in longitudinal reinforcement ratio.

For the same longitudinal rebar ratio, specimens with GFRP rebars, outperformed their conventional steel rebars. Improved load-bearing capacities by 65%, 25% and 11% were observed for low, medium and high reinforcement ratios, respectively.

With regard to deflection corresponding to the peak load, higher reinforcement ratios contributed to the occurrence of peak loads ant larger deflections with the rate increasing with the reinforcement ratio.

Linear regression models were established to estimate the fracture energy of the specimens in terms of different ratios of the clear span.

Fracture energy of specimens with conventional steel rebar was notably higher than their GFRP counterparts especially in the post-yield region.

Nonlinear regression models were also proposed which successfully captured the load-deflection behavior of the beams with coefficient of determination close to unit.

Funding

This research did not receive any specific grant from funding agencies in the public, commercial, or not-for-profit sectors.

Conflicts of interest

The authors declare that they have no known competing financial interests or personal relationships that could have appeared to influence the work reported in this paper.

References

[1] Luhar S, Cheng TW, Nicolaides D, Luhar I, Panias D, Sakkas K. Valorisation of glass wastes for the development of geopolymer composites – Durability, thermal and microstructural properties: A review. Constr Build Mater 2019. https://doi.org/10.1016/j.conbuildmat.2019.06.169.

[2] Visintin P, Sturm AB, Mohamed Ali MS, Oehlers DJ. Blending macro- and micro-fibres to enhance the serviceability behaviour of UHPFRC. Aust J Civ Eng 2018. https://doi.org/10.1080/14488353.2018.1463608.

[3] Pourbaba M, Joghataie A, Mirmiran A. Shear behavior of ultra-high performance concrete. Constr Build Mater 2018. https://doi.org/10.1016/j.conbuildmat.2018.06.117.

[4] Ahmed Shaikh F, Arel H. Effects of curing types, fly ash fineness and fibre lengths on mechanical and impact properties of steel fibre reinforced concretes. Aust J Civ Eng 2020. https://doi.org/10.1080/14488353.2020.1771663.

[5] Venkateshwaran A, Tan KH, Li Y. Residual flexural strengths of steel fiber reinforced concrete with multiple hooked-end fibers. Struct Concr 2018. https://doi.org/10.1002/suco.201700030.

[6] Feng J, Sun WW, Wang XM, Shi XY. Mechanical analyses of hooked fiber pullout performance in ultra-high-performance concrete. Constr Build Mater 2014. https://doi.org/10.1016/j.conbuildmat.2014.07.049.

[7] Ibrahim MA, Farhat M, Issa MA, Hasse JA. Effect of material constituents on mechanical & fracture mechanics properties of ultra-high-performance concrete. ACI Struct J 2017. https://doi.org/10.14359/51689717.

[8] Hao, Q. D., Wang, B., & Ou JP. Fibre reinforced polymer rebar's application to civil Engineering. Concrete 2006;9:38–40.

[9] Yoo DY, Banthia N, Yoon YS. Flexural behavior of ultra-high-performance fiber-reinforced concrete beams reinforced with GFRP and steel rebars. Eng Struct 2016. https://doi.org/10.1016/j.engstruct.2015.12.003.

[10] Ahangarnazhad BH, Pourbaba M, Afkar A. Bond behavior between steel and Glass Fiber Reinforced Polymer (GFRP) bars and ultra high performance concrete reinforced by Multi-Walled Carbon Nanotube (MWCNT). Steel Compos Struct 2020. https://doi.org/10.12989/scs.2020.35.4.463.

[11] de Sá FRG, Silva F de A, Cardoso DCT. Tensile and flexural performance of concrete members reinforced with polypropylene fibers and GFRP bars. Compos Struct 2020. https://doi.org/10.1016/j.compstruct.2020.112784.

[12] Dev A, Chellapandian M, Prakash SS, Kawasaki Y. Failure-mode analysis of macro-synthetic and hybrid fibre-reinforced concrete beams with GFRP bars using acoustic emission technique. Constr Build Mater 2020. https://doi.org/10.1016/j.conbuildmat.2020.118737.

[13] Patil GM, Chellapandian M, Suriya Prakash S. Effectiveness of hybrid fibers on flexural behavior of concrete beams reinforced with glass fiber-reinforced polymer bars. ACI Struct J 2020. https://doi.org/10.14359/51725844.

[14] Liu S, Wang X, Ali YMS, Su C, Wu Z. Flexural behavior and design of under-reinforced concrete beams with BFRP and steel bars. Eng Struct 2022;263:114386.

[15] El-Sayed TA, Algash YA. Flexural behavior of ultra-high performance geopolymer RC beams reinforced with GFRP bars. Case Stud Constr Mater 2021. https://doi.org/10.1016/j.cscm.2021.e00604.

[16] Betschoga C, Tung ND, Tue NV. Investigations on the influence of boundary and loading conditions on the shear resistance of FRP concrete beams without shear reinforcement. Compos Struct 2021. https://doi.org/10.1016/j.compstruct.2020.113335.

[17] Dadmand B, Pourbaba M, Sadaghian H, Mirmiran A. Effectiveness of steel fibers in ultra-high-performance fiber-reinforced concrete construction. Adv Concr Constr 2020. https://doi.org/10.12989/acc.2020.10.3.195.

[18] ASTM International. West Conshohocken P. ASTM C469 / C469M-14, Standard Test Method for Static Modulus of Elasticity and Poisson's Ratio of Concrete in Compression. 2014.

[19] ASTM International, West Conshohocken P. ASTM C1609 / C1609M-19a, Standard Test Method for Flexural Performance of Fiber-Reinforced Concrete (Using Beam With Third-Point Loading). 2019.

[20] A. KG. Impact of age and size on the mechanical behavior of an ultra-high performance concrete (Doctoral dissertation). Michigan Technol Univ 2004.

[21] (KCI) KCI. Concrete Design Code and Commentary. Kimoondang Publ Co Seoul, Repub Korea 2007;327.

[22] Graybeal BA. Compressive behavior of ultra-high-performance fiber-reinforced concrete. ACI Mater J 2007. https://doi.org/10.14359/18577.

[23] Graybeal, B. A., & Stone B. Compression response of a rapid-strengthening ultra-high performance concrete formulation (No. FHWA-HRT-12-065). United States Fed Highw Adm Off Infrastruct Res Dev 2012.

[24] Lee SC, Oh JH, Cho JY. Compressive behavior of fiber-reinforced concrete with end-hooked steel fibers. Materials (Basel) 2015. https://doi.org/10.3390/ma8041442.

[25] Alsalman A, Dang CN, Prinz GS, Hale WM. Evaluation of modulus of elasticity of ultra-

high performance concrete. Constr Build Mater 2017. https://doi.org/10.1016/j.conbuildmat.2017.07.158.

[26] Haber ZB, Varga ID la, Graybeal BA, Nakashoji B, El-Helou R. Properties and Behavior of UHPC-Class Materials. Report No FHWA-HRT-18-036. 2018.

[27] Suksawang N, Wtaife S, Alsabbagh A. Evaluation of elastic modulus of fiber-reinforced concrete. ACI Mater J 2018. https://doi.org/10.14359/51701920.